ORIGINAL ARTICLE

# Influence of Phospholipids Structure on the Physicochemical Properties and In Vitro Digestibility of Lactoferrin-Loaded Liposomes

Jiawei Zhang[1] · Jianzhong Han[1] · Aiqian Ye[1,2] · Weilin Liu[1] · Mengmeng Tian[1] · Yujie Lu[1] · Kunrong Wu[1] · Jing Liu[1] ·
Ma Peizhan Lou[1]

## Abstract
The instability of liposomal delivery system during passaging through the gastrointestinal tract (GIT) stimulates a demand to find a stable liposome. This research studied the implications of different types of phospholipids (different fatty acid chain length and saturation, various head group) on liposomal physiochemical properties and stability in the human GIT. The micropolarity of liposomal membrane increased with the decrease of chain lengths of phospholipids, while the morphology observation revealed that the liposomes formed by different phospholipids showed similar in appearance and shapes. The liposomes formed by $C_{20:0}$ deformed more severely in simulated gastric fluid, while others exhibited slight changes in the membrane structure. In simulated intestinal fluid, pancreatic lipase and phospholipase $A_2$, synergized with bile salts, damaged the bilayers structure of all liposomes, with the entrapped lactoferrin release and hydrolysis. Although the various phospholipid structures lead to some difference on the physicochemical properties (size and micropolarity), the enzymic influence displayed more significance during in vitro digestion compared to the types of wall materials. Current results could provide valuable information for the development of more stable and reliable food-grade liposomes in the GIT.

**Keywords** Liposomes · Phospholipids · In vitro digestion · Structure

## Introduction

Liposomes are self-assembling and cell-resembling colloidal delivery systems, which comprise a bilayer formed by amphiphilic molecules and an aqueous core [1]. They can incorporate hydrophobic molecules in the bilayer membrane and encapsulate hydrophilic compounds in the aqueous internal cavity and offer a promising chance to enhance the entrapped cargo stability [2, 3]. Compared with traditional delivery systems, such as nanoemulsion, nanosphere, microcapsule, or with the new delivery systems like W1/O/W2 emulsion gels [4], Fish oil emulsions [5], liposomes show multiple advantages including biocompatibility, biodegradability and nontoxicity [6]. Liposomes have been applied in protecting and controlling the release of functional compounds in pharmaceutics, cosmetics and agriculture [7, 8]. Recently,

✉ Weilin Liu
lwl512@zjgsu.edu.cn

Jiawei Zhang
842665541@qq.com

Jianzhong Han
hanjz99@zjgsu.edu.cn

Aiqian Ye
a.m.ye@massey.ac.nz

Mengmeng Tian
971468842@qq.com

Yujie Lu
935014988@qq.com

Kunrong Wu
383260457@qq.com

Jing Liu
1291838349@qq.com

Ma Peizhan Lou
1018525663@qq.com

[1] School of Food Science and Biotechnology, Zhejiang Gongshang University, Hangzhou 310018, China

[2] Riddet Institute, Massey University, Private Bag 11 222, Palmerston North 4442, New Zealand

there is extensive published information on liposomes loaded bioactive compounds in food and nutrition, such as flavonoids (quercetin, luteolin, kaempferol) [9], antioxidative peptide [10] and curcumin [11], and vitamins like vitamins E and C [12, 13].

The physicochemical and biological properties of liposomes can be affected by both their surface properties and wall compositions. Recently, increasing studies tended to modify the liposomal surface by coating polysaccharides [14], polyethylene glycol [15] and protein [16] on the surface of vesicles, to improve the functionality of liposomes. However, surface modifiers may interact with food or encapsulated molecules in liposomes. On the other hand, the structure of phospholipids, which is the fundamental and the most often used wall materials of liposomes [17], crucially influence the liposomal properties. Phospholipids are amphiphilic molecules in which hydrophilic head group and hydrophobic acyl chains are linked to the glycerin. The variation in head groups, aliphatic chains and the saturation of fatty acids leads to the difference of functionality of liposomes. María and coworkers reported that the entrapment efficiency of suramin decreased with the increase in the chain length of dipalmitoylphosphatidylcholine ($C_{12}$, $C_{14}$, $C_{16}$, $C_{18}$) in multilamellar liposomes [18]. Zhao et al. reported that liposomes formed by phosphatidic acid (PA) and phosphatidylinositol (PI) showed higher absolute zeta potential than liposomes formed by phosphatidylethanolamine (PE) [19]. However, there is no systematic information on the microstructure and permeability of liposomes formed by different structured phospholipids.

Recently, studies related to the digestion fate of liposomes in the human gastrointestinal (GI) tract have attracted much attention [20–22]. Efforts also have been risen to improve the bioaccessibility and bioavailability of entrapped ingredients by surface modification of liposomes [21, 23]. Our previous studies have conducted an exhaustive characterization of liposomes prepared from phospholipids derived from soybean and milk fat globule membrane and illustrated systematically their structural integrity during in vitro digestion [23, 24]; the effects of cholesterol incorporation in bilayers and lactoferrin decoration on external surface on the in vitro infant intestinal digestion behavior of liposomes also have been studied [25, 26]. Besides, liposomes formed by different phosphocholines have been fabricated to deliver calcein to study the release kinetics in the gastrointestinal tract in humans [27]. The characteristics of liposomes composed of soybean lecithin and hydrogenated soybean lecithin during in vitro digestion have been studied [28], and it is shown that the digestion behavior of 1-palmitoyl-2-oleoyl-snglycerol-3-phosphocholine (POPC), 1-palmitoyl-2-hydroxy-snglycerol-3-phosphocoline (LPC), and 1,2-didodecanoyl-snglycero-3-phosphocholine (DLPC) in

different bile salt concentrations had some differences [29]. Bioactive molecules loaded liposomes were even fortified into the real food to regulate food digestibility [30]. Whereas, the linkage of phospholipids structure and liposomal digestibility, which may offer the various possibility in vitro stability, is unknown and needs deeper exploration.

Therefore, present study aimed to extend our previous work and to provide more information on the stability of liposomes with different types of phospholipids as wall materials under GI tract conditions. Liposomes were prepared using different chain lengths ($C_{16:0}$, $C_{18:0}$, $C_{20:0}$), different saturations ($C_{18:0}$, $C_{18:1}$, $C_{18:2}$, $C_{18:3}$) and different head groups of phospholipids. The particle size, zeta potential, micropolarity of membrane and morphology of the liposomes before and after in vitro digestion were investigated. In order to evaluate the membrane stability of the liposomes, the release of the encapsulated cargos (lactoferrin, LF) release and the structure integrity of the liposomes were also evaluated.

## Materials and Methods

### Materials

1,2-dipalmitoyl-sn-glycero-3-phosphocholine ($C_{16:0}$, DPPC), 1,2-distearoyl-sn-glycero-3-phosphocholine ($C_{18:0}$, DSPC), 1,2-diarachidoyl-sn-glycero-3-phosphocholine ($C_{20:0}$, PC), 1,2-dioleoyl-sn-glycero-3-phosphocholine ($C_{18:1}$, DOPC), 1,2-dilinoleoyl-sn-glycero-3-phosphocholine ($C_{18:2}$, DLPC), 1,2-dilinolenoyl-sn-glycero-3-phosphocholine ($C_{18:3}$, PC), 1,2-distearoyl-sn-glycero-3-phosphate (sodium salt) ($C_{18:0}$, PA), 1,2-distearoyl-sn-glycero-3-phosphoethanolamine ($C_{18:0}$, PE), and 1,2-distearoyl-sn-glycero-3-phosphoinositol ($C_{18:0}$, PI) with purity >99% were purchased from Avanti Polar Lipids (Alabaster, AL, USA). Lactoferrin (LF, ≥90%) was purchased from Tatua Co-operative Dairy Company Ltd. (Morrinsville, New Zealand). Octadecylamine (≥99.0%), cholesterol (≥99.0%), Pyrene (≥99.0%), bile extract porcine, pancreas (4 × USP), pepsin (50 U/mg) and α-amylase (50 U/mg) were obtained from Sigma-Aldrich (Oakville, ON, Canada). All other chemicals were of analytical grade and were provided from Sigma-Aldrich (Oakville, ON, Canada).

### Preparation of Lactoferrin-Loaded Liposomes

Liposomes were prepared using the thin layer dispersion method as described in our previous study [31]. In brief, phospholipids with different chain lengths ($C_{16:0}$, $C_{18:0}$, $C_{20:0}$), saturations ($C_{18:0}$, $C_{18:1}$, $C_{18:2}$, $C_{18:3}$) and head groups (PA, DSPC, PE, PI) were well-dissolved mixed with cholesterol and octadecylamine in chloroform in a mass ratio of 0.5:9:0.5, respectively. The organic solvent was evaporated and a thin film was formed at 55 °C under vacuum in a rotary

evaporator (RE5298; Yarong Biochemical Instrument Factory, Shanghai, China). The dried lipid film was rehydrated with phosphate-buffered saline (PBS, pH 7.2, 0.1 M) containing 0.2 mg/mL LF to obtain a LF-loaded liposomal suspension, with a lipid (phospholipid/cholesterol) concentration of 0.244 mg/mL.

## Physic-Chemical Properties of Lactoferrin-Loaded Liposomes

### Dynamic Light Scattering

The dynamic light scattering (DLS) technique was used to determine the average diameter and surface charge of the liposomes formed by different phospholipids. The measurements were performed on a Malvern Zetasizer Nano ZSP instrument (Malvern Instruments Ltd., Malvern, Worcestershire, UK) at 25 °C with the scattering angle 173°. The relative refractive index and the absorption of the phospholipid were 1.120 and 0.001, respectively. All data were calculated as the average value based on at least triplicated measurements.

### Micropolarity

The method of Galletti et al. [32] and a HITACHI spectrofluorometer F-7000 (Tokyo, Japan) were used to evaluated liposomal membrane micropolarity, which equipped with excitation and emission polarization filters. A stock solution of a fluorescent probe was prepared by dissolving 607.00 mg pyrene in 100 mL ethanol in a brown volumetric flask. 0.012 mL stock solution of a fluorescent probe was blown by nitrogen, and then 1.20 mL liposomal suspension with different wall structure were added and mixed in a water bathed for 30 min (37 °C, 95 rpm), followed by adding 1.80 mL liposomes to the mixture. Pyrene showed five emission peaks when excited at 334 nm. The intensity ratio ($I_1/I_3$) of peak 1 (about 375 nm) to peak 3 (about 385 nm) served as a measurement of the micropolarity. All experiments were performed at 25 °C and all determinations were background subtracted using an appropriate blank.

### Morphology

The morphology of liposomes was observed by Transmission electron microscopy (TEM) and Atomic force microscope (AFM). For AFM, liposomal samples were diluted 10-folds in PBS before observation. A droplet of liposomal solution was dropped onto the surface of a freshly cleaved mica substrates. The sample on the mica sheet was analyzed on an AFM (Agilent 5500, Agilent Technologies, Santa Clara, CA, USA) with a silicon cantilever under the force constant of 0.58 N m$^{-1}$ in tapping mode at room temperature.

A droplet of liposomal suspension was dropped on a copper grid for 20 min and then stained the grid with uranyl acetate solution (2% in acetone) for 4 min followed by removing the excess liquid using a filter paper. The morphology of the LF-loaded liposomes was recorded under a TEM (CM10, Philips, Eindhoven, Netherlands) at 25,000 magnifications.
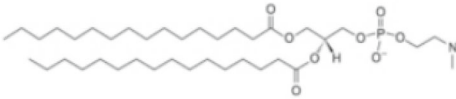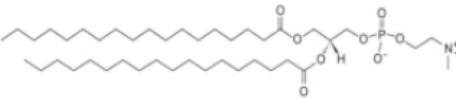
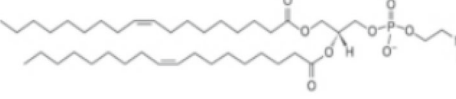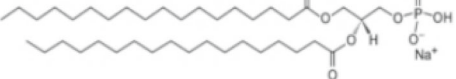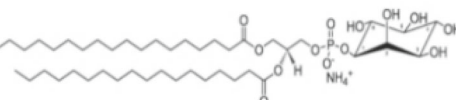## In Vitro Digestion of Lactoferrin-Loaded Liposomes
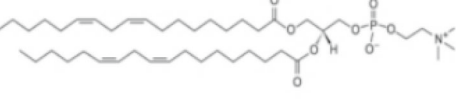
Simulated salivary fluid (SSF), simulated gastric fluid (SGF) and simulated intestinal fluid (SIF) were prepared as the report of Minekus et al. [33].1 mL liposomes with different chain lengths ($C_{16:0}$, $C_{18:0}$ and $C_{20:0}$) were pre-heated in a shaking water bath (95 rpm/min) at 37 °C for 25 min and then mixed with SSF in a volume ratio of 1:1 ($v/v$) by adjusting the pH to 7.0. The digestion procedure started at the addition of $\alpha$-amylase (75 U/mL). After 2 min of oral digestion, 2 mL SGF containing pepsin (2000 U/mL) was added to the mixture and the pH was quickly adjusted to 3.0 using 0.05 M HCl, and then the mixture was digested in a shaking water bath (95 rpm/min) at 37 °C for 2 h. Then the gastric-digested liposomal solution was mixed with 4 mL SIF containing pancreatin (100 U/ml) and bile salts (10 mM) and the pH was adjusted to 7.0 and digested for 2 h.

## Digestion Behaviors of Lactoferrin-Loaded Liposomes with Different Structure of Phospholipids

### Changes in Size Distribution and Zeta Potential

Changes in size distribution and zeta potential of liposomes with different structure of phospholipids were observed at the end of in vitro SGF and SIF digestion using NanoSight tracking analysis (NTA, NS300 Malvern Instruments Ltd., Malvern, UK) instrument and DLS. NTA measurements with respect to size distribution in a three-dimensional (3D) plots (size, concentration and light intensity) was equipped with a sample chamber with a 640 nm laser and a Viton fluoroelastomer O-ring. The samples were diluted 5-folds in PBS before being injected in the chamber with syringes until the samples reached to the tip of the nozzle. Video of particle motion was recorded at 30 frames per second, and the samples were measured for 60 s with fixed shutter and gain adjustments. At least 1800 tracks were completed during video analysis using NanoSight software NTA version 3.1 Build 3.1.45 (NanoSight Ltd., Malvern, UK). Particle distributions were calculated from particle tracks using Stokes- Einstein equation. The average size and zeta potential of the liposomes with different wall materials digested in SGF and SIF were obtained by DLS technology mentioned above.

**Table 1** The Size, PDI, Zeta, Micropolarity of LF liposomes formed by different structure of phospholipid

| | | Phospholipids structure | Size/nm | PDI | Zeta/mV | Micropolarity |
|---|---|---|---|---|---|---|
| Chain Length | 16:0 | | 365.3±60.2 | 0.505±0.1 | 8.1±1.7 | 1.6±0.1 |
| | 18:0 | | 721.3±42.0 | 0.683±0.1 | 9.2±1.5 | 1.5±0.1 |
| | 20:0 | | 438.8±34.2 | 0.516±0.1 | 8.2±1.3 | 1.4±0.1 |
| Saturation | 18:1 | | 804.9±10.1 | 0.578±0.1 | 9.5±0.5 | 1.3±0.3 |
| | 18:2 | | 450.6±50.0 | 0.505±0.1 | 8.6±2.0 | 1.3±0.1 |
| | 18:3 | | 689.8±69.3 | 0.597±0.1 | 9.7±0.2 | 1.2±0.2 |
| Head group | PA | | 343.1±79.1 | 0.484±0.1 | -11.6±1.5 | 1.3±0.1 |
| | DSPC | | 721.3±42.0 | 0.683±0.1 | 9.2±1.5 | 1.5±0.1 |
| | PE | | 242.5±76.5 | 0.563±0.1 | 10.1±1.7 | 1.3±0.1 |
| | PI | | 300.0±20.6 | 0.581±0.1 | -14.1±1.9 | 1. 5±0.1 |

## Steady State Fluorescence Measurements

The membrane micropolarity, which indicates the structure integrity of liposomal membrane during digestion,

**Fig. 1** Size distribution curve of liposomes formed by different structure ▶ of phospholipids. **a** Different chain lengths; **b** different saturations; **c** different head groups
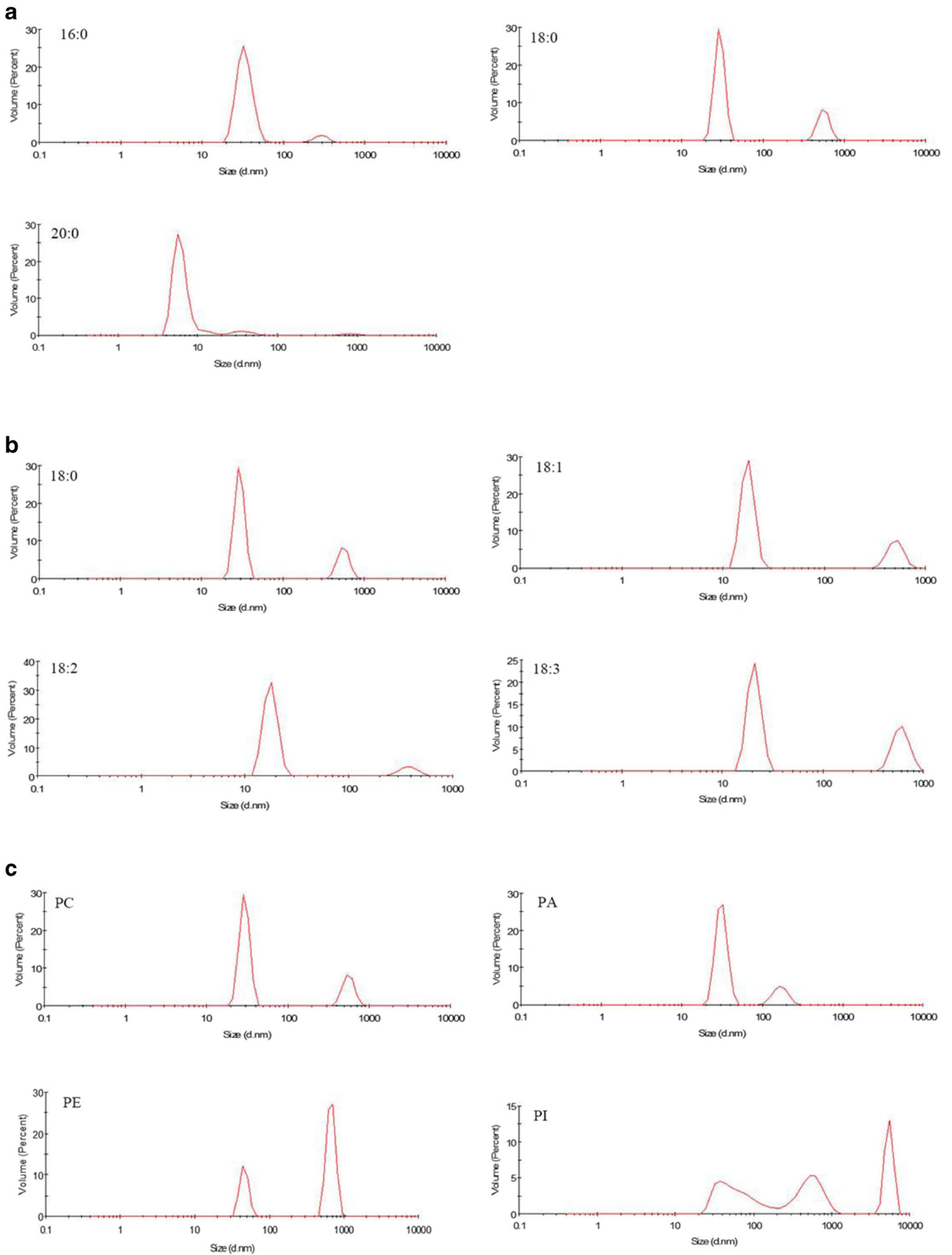
was assessed using a fluorescent pyrene probe. Digested samples were recorded by measuring the fluorescent peak ratio $I_1/I_3$ of pyrene, as referred in 2.3.2.

## Changes in Microstructure

TEM (CM10, Philips, Eindhoven, Netherlands) was used to provide visual confirmation of the structure changes of liposomes during in vitro digestion. The samples digested in SGF and SIF for 120 min were monitored as described in 2.3.3.

## Protein Hydrolysis

The digestion of protein was examined by sodium dodecyl sulphate polyacrylamide gel electrophoresis (SDS-PAGE), as reported by Ye, et al. [20]. Liposomes formed by $C_{16:0}$, $C_{18:0}$ and $C_{20:0}$ before and after digestion in SGF and in SIF for 120 min were placed in Eppendorf vials and heated in a boiling water bath (~ 95 °C) for 2 min to inactive the enzyme before being treated with sample buffer (0.5 M Tris, 2.0% SDS, 0.04% Coomassie Brilliant Blue G-250 and 0.1 M dithiothreitol, pH 6.8) in a volume ratio of 1:1 followed by heating in the boiling water bath (95 °C ~ 100 °C) for 5 min. After cooling to room temperature, 15 μL samples were loaded on to a fresh gel (4% stacking gel and 16% resolving gel) and were run for 30 min in a Mini-Protean system (Bio-Rad Laboratories) at 70 V using a Bio-Rad power supply unit (Model 1000/500, Bio-Rad Laboratories, Richmond, CA, USA), and then was run at 110 V for 15 min. The gel was stained using staining solution (0.03% Coomassie Blue R-250, 10% glacial acetic acid and 20% isopropanol) for about 40 min and de-stained in de-staining solution (10% glacial acetic acid, 10% isopropanol) until the background faded sufficiently, followed by scanning on a molecular imager (Universal Hood II, Bio-Rad Laboratories, Richmond, CA, USA).

## Data Analysis

All measurements were repeated at least three times. The results were evaluated statistically with SPSS software version 18.0 (IBM Corp. Chicago, IL, USA). Statistical analysis was performed by one-way analysis of variance with Tukey's honestly significant difference post hoctest. The level of signifizcance was set at $P < 0.05$. All data were expressed as means ± standard deviations.

## Results and Discussion

### Characterization of LF-Loaded Liposomes

The average diameter of the liposomes formed by $C_{18:0}$ (721.3 ± 42.0 nm) was much larger ($p < 0.05$) than the size of liposomes formed by $C_{16:0}$ (365.3 ± 60.2 nm) and $C_{20:0}$ (438.8 ± 34.2 nm) (Table 1). Among the liposomes prepared from different head groups of phospholipids, it can be apparently observed that the average diameter of liposomes formed by DSPC was almost twice as big as the liposomes formed by PA, PE and PI. The effect of difference in wall materials on the zeta potential of liposomes was not obvious (± 6.0 mV~16.0 mV), whereas, it was noteworthy observed that the liposomes formed by PA and PI exhibited a negative charge, while others were positive charge. The micropolarity values gradually decreased with the increase in relative molecular mass, which showed that the micropolarity of liposomes formed by $C_{16:0}$ (1.6 ± 0.1) was larger ($p < 0.01$) than the liposomes formed by $C_{18:0}$ (1.5 ± 0.1) and $C_{20:0}$ (1.4 ± 0.1). Besides, the micropolarity of liposomes formed by different saturations of phospholipids have a tendency to decrease as the saturations of phospholipids increased. The size distribution curve showed a wild distribution in liposomes formed by PI while others' showed a narrow distribution. Almost every samples contain two distribution intervals in the curve (Fig. 1), which corresponding to the results of PDI (Table 1).

The present results showed that the wall material structure had slight effect on the average particle size. Negative zeta potentials of PA and PI liposomes were due to the negative charge head groups. A larger $I_1/I_3$ serves as greater polarity. The polarity of liposomes formed by different phospholipids may be attributed to the lower net van der Waals interaction between hydrocarbon chains for shorter acyl chains, namely, the shorter the acyl chains length, the weaker interaction of hydrophobic between acyl chain length [34]. Therefore, the decrease in chain lengths leaded to the increase in the micropolarity of liposomes. Besides, the increase in unsaturation degree led to more hydrophobic, duing to their more crooked spatial arrangement and increasing in van der Waals interactions and consequently, decreasing the micropolarity [35].

### Morphology

AFM images of liposomes formed by different type of phospholipids were shown in Fig. 2. The Polymer disparity index

**Fig. 2** Atomic force microscope (AFM) images of lactoferrin-loaded ▶ liposomes formed by different structure of phospholipids. **a** Different chain lengths; **b** different saturations; **c** different head groups

**a**

16:0  18:0  20:0

**b**

18:0  18:1

18:2  18:3

**c**

PA  DSPC

PE  PI
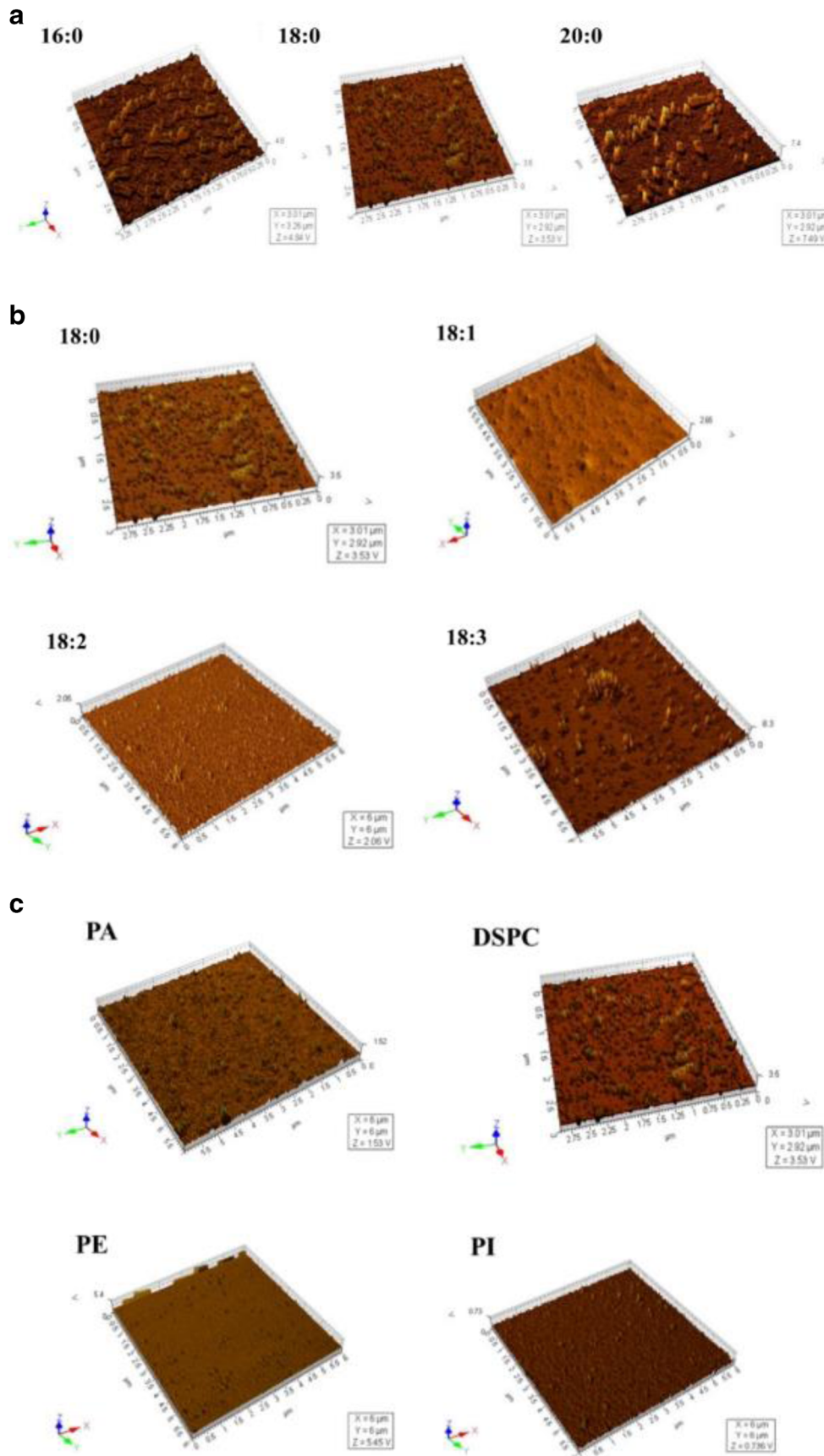
(PDI) measured by DLS could reflect to the aggregation of liposome particles. The larger in PDI, the more aggregation of particles. Compared to $C_{16:0}$ (PDI = 0.505) and $C_{20:0}$ (PDI = 0.516) liposomes, LF-loaded liposomes formed by $C_{18:0}$ (PDI = 0.683) exhibited less uniformed, with both very small and large particles being observed in Fig. 2a. The saturations of phospholipids seemed to influence the size distributions of liposomes, since some big aggregation could be found in the images of $C_{18:3}$ vesicles (Fig. 2b). Besides, it was found that the liposomes formed by DSPC showed rough surface with some large particles gathered together, while liposomes formed by PA, PE and PI displayed smoother in appearance and showed better distribution (Fig. 2c). TEM images in Fig. 3 revealed that most liposomes were multi-lamellar vesicles (Fig. 3b and c) and the size was about 400–800 nm, which was in accordance with the size measurement using DLS (Table 1). The vesicles appeared to be similar in shapes for the liposomes formed by different type of phospholipids. For example, in terms of the different chain length of phospholipids (Fig. 3a), the image of liposome formed by $C_{16:0}$, $C_{18:0}$ and $C_{20:0}$ all showed spherical in shape with smooth and intact surface (Fig. 3a). Liposomes formed by $C_{18:2}$ seemed smaller than others, which were consistent with the size detection.

The results of AFM demonstrated that different structure of wall materials may cause differences in size, shape and size distribution of liposomes. However, from the more detailed TEM observation, it seems that the liposomes formed by different type of phospholipids have little differences in their structure, which was similar to the others' observation, which found that the shape of liposomes would be slightly influenced by the utilization of different phospholipids (Hydrogenated Phospholipon 90H and non-hydrogenated soy phosphatidylcholine Lipoid S100) [36]. In addition, the TEM images confirmed to the report that the amphiphilic phospholipid membranes can assemble into vesicles with different structures including unilamellar and multilamellar, which is a crystalline bilayer state [37].

## Changes in Size Distribution and Zeta Potential of Liposomes during In Vitro Digestion

All the liposomes formed by different chain lengths of phospholipids ($C_{16:0}$, $C_{18:0}$ and $C_{20:0}$) exhibited wider size distributions and greater aggregation after SGF digestion, with the size being larger than 2000 nm and remarkably bigger ($p < 0.01$) than the original samples (300 ~ 800 nm). The particles after SIF incubation showed narrower distributions and the sizes were around half of the samples digested in SGF (Fig. 4). In agreement with DLS measurement (data inserted in the images), the mean diameters obtained by NTA had similar patterns. For example, liposomes formed by $C_{20:0}$ digested in SGF and SIF were 2639.0 ± 97.0 nm and 1110.6 ± 57.8 nm, respectively. However, they were still larger

($p < 0.05$) than that of the original liposomes (438.8 ± 34.2 nm). The zeta potential of undigested liposomes showed a positive charge (8.1 mV ~ 9.2 mV), while they displayed a negative charge after SGF digestion (−14.6 ~ −14.2 mV), and further ($p < 0.01$) decreased to more negatively (−19.1 ~ −17.2 mV) after SIF digestion.

The increase in average sizes of liposomes in SGF for may be due to the aggregation of particles at low pH environment, supporting by the 3D images from NTA observation. The ionic strength of diluent would change the direction of the lipid head group in the liposome surface region. At low ionic strengths, even at deionized water, the phosphatidyl groups which contacted with negative charge are located at the outer portion of the head group region [38]. After SIF digestion, the liposomal membrane is destroyed by the effect of bile salts and lipolytic enzymes. The intact structure of vesicles was damaged to small fragments and the released LF was also hydrolyzed by the trypsin in the pancreatic enzymes, leading to the smaller particle size under the intestinal conditions. The increase in the negative charge of the liposomes could be contributed to the following two factors. 1) Phospholipase $A_2$, contains in pancreatin, catalyzes the hydrolysis of the ester linkage of the sn-2 acyl chain of phospholipids, yielding 2-acyl lysophospholipids, which have a high negative charge. 2) The bile salts would be incorporated into bilayers, making the polar head groups of phospholipids apart [38], and thus increase the negative change of the vesicles.

DLS is the preferred technique to routinely determine the size of nanoparticles, because it yields relatively accurate and consistent results that can be obtained in a rather short period of time [39]. DLS is an established method for bulk analysis of liquid samples, which is intensity-based size distribution, and measures the fluctuations in the intensity of the light scattered from the particles in a sample [40]. The small amounts of large aggregates would impede the size determination if the main component exhibits a distinctly smaller size [41]. The NTA is able to identify and track individual nanoparticles moving under Brownian motion and relates the movement to a particle size. Therefore, the diameter determined by DLS usually is bigger than that measured by NTA. For instance, the size of undigested liposomes formed by $C_{18:0}$ was 721.3 ± 42.0 nm measured by DLS, around 450 nm obtained by NTA.

## Changes in Micropolarity of Liposomal Membrane During In Vitro Digestion

The changes in the $I_1/I_3$ ratio for pyrene in liposomes formed by different chain length of phospholipids before and after digestion were presented in Fig. 5a. The $I_1/I_3$ ratio of original liposomes mad by $C_{16:0}$, $C_{18:0}$ and $C_{20:0}$ decreased with the increasing of phospholipids chain length, and after SGF digestion, the tendency of $I_1/I_3$ ratio of the liposomes formed by $C_{16:0}$, $C_{18:0}$ and $C_{20:0}$ was similar with original liposomes. It

**Fig. 3** Transmission electron microscopy (TEM) images of lactoferrin-loaded liposomes formed by different structure of phospholipids. **a** Different chain length of phospholipids; **b** different saturation of phospholipids; **c** different head group of phospholipids
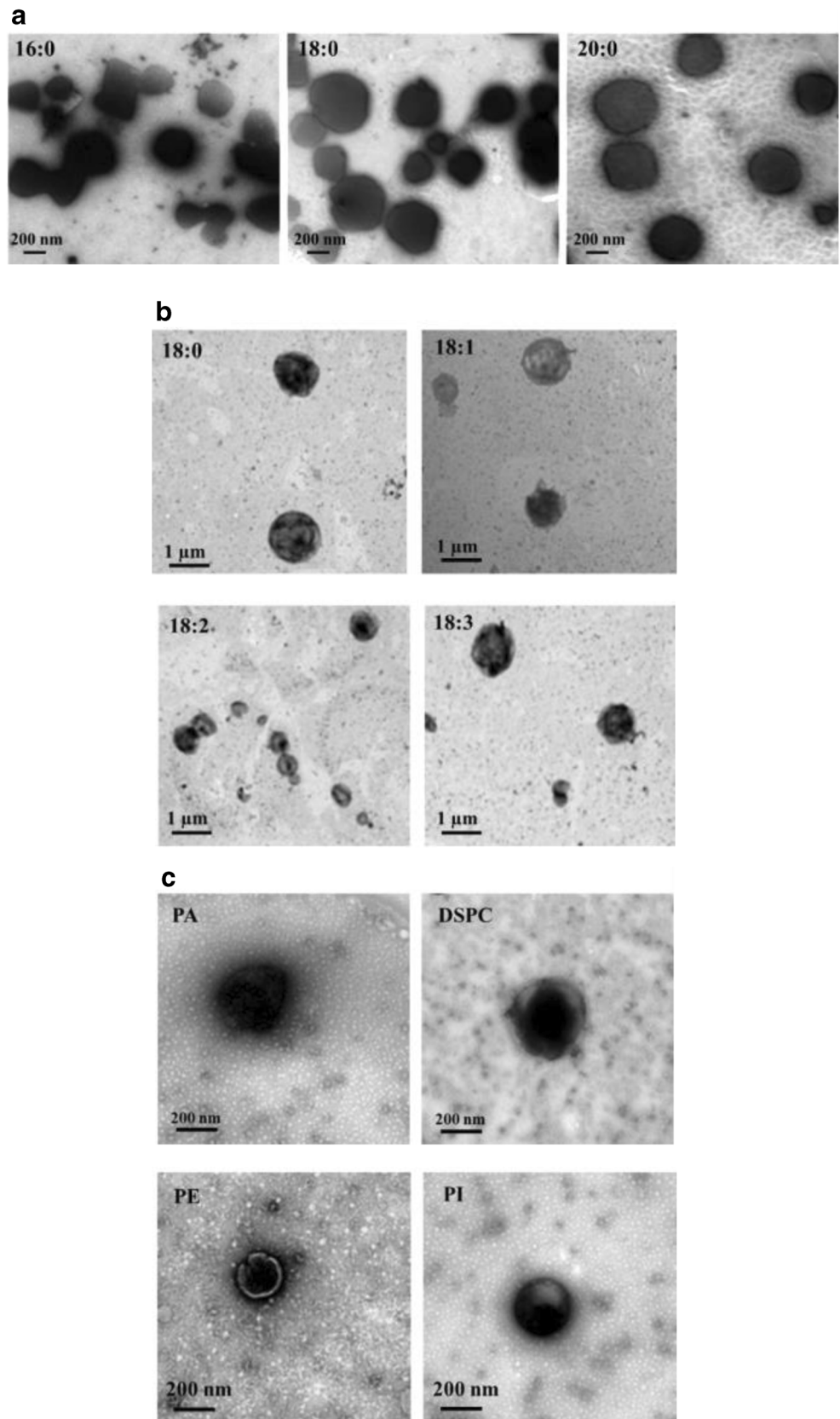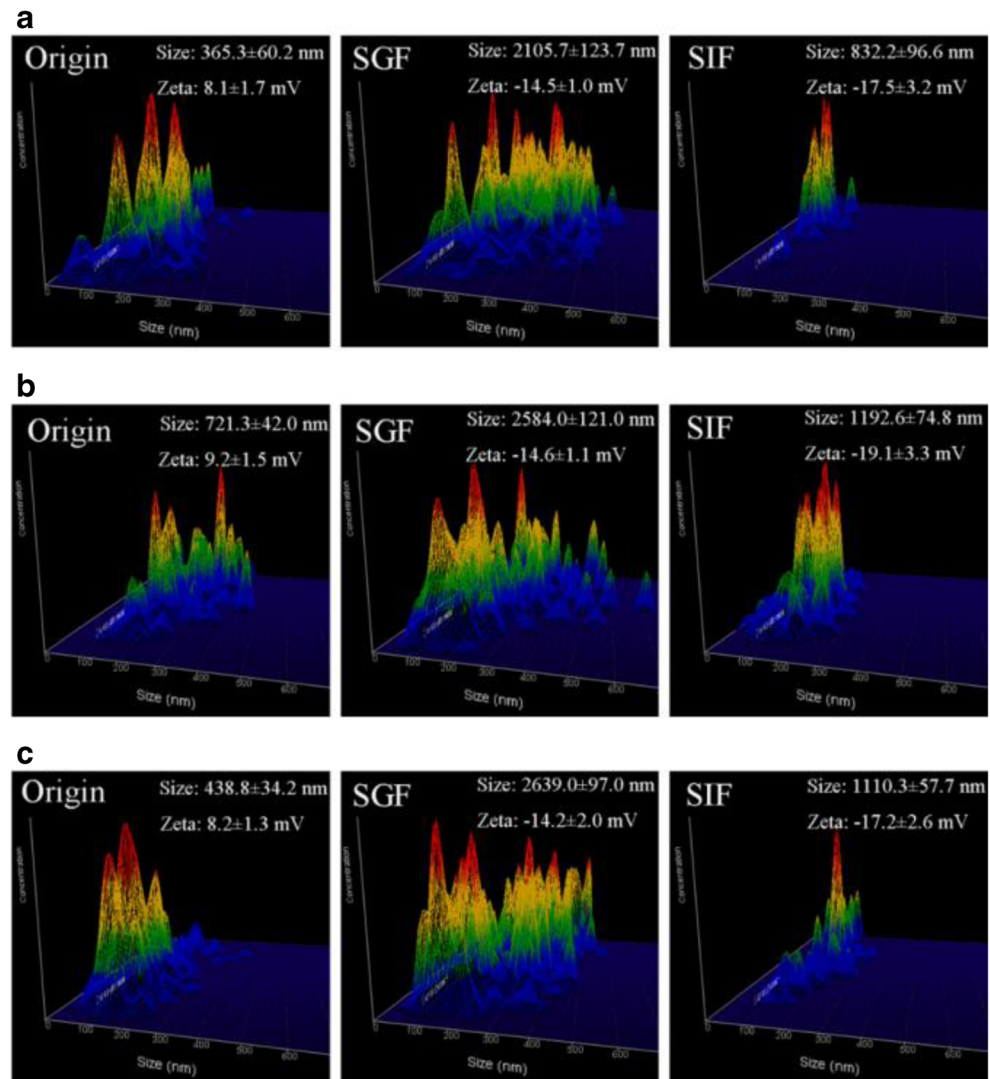
was noteworthy that the value of $I_1/I_3$ decreased sharply ($p < 0.05$) after SGF digestion, however, these values in the following SIF digestion slight changes, with similar values among the three kinds of chain lengths liposomes. Pyrene would localize in the hydrophobic interfacial region of the bilayer membranes, and the monomer forms excimers in a diffusion-limited reaction (Fig. 5b).

The $I_1/I_3$ ratio is supposed to increase quickly at the environment where pyrene changes from highly hydrophobic to more hydrophilic (formed in the presence of a polar modifier) [42]. The significant decrease ($p < 0.05$) in $I_1/I_3$ values of liposomes after stomach digestion (compared to the original) indicated the reduce of bilayer membrane fluidity. Since the pH of the medium (SGF, pH 3.0) was lower than the inside environment of liposomes (pH 7.0), it could form a osmotic pressure difference between two sides of liposomal membrane, which may make the phospholipids arranging more compact [43, 44]. Therefore, the liposomal membrane fluidity became lower and the pyrene probe preferred to stay in the

area of hydrophobic fatty acid chains of phospholipids rather than moving around, leading to $I_1/I_3$ ratios apparently decreased. In intestine, the intact structure of liposomes was damaged and the well-organized bilayers became disorder and even hydrolyzed to the intermediate hydrolysis products, lysophospholipids, and the end products, such as non-esterified fatty acids and glycerophospho compound, which have smaller polarity than their "mother lipids" (phospholipid). Thus, the values of $I_1/I_3$ were all smaller than the undigested liposomes.

## Liposomal Membrane Integrity

The microstructure changes of liposomes were monitored using TEM (Fig. 6). All the liposomes with different chain lengths exhibited more irregular structures with rougher surfaces after digestion in SGF, compared to the original samples (Fig. 3a), and the liposomal deformation of $C_{20:0}$ was the most serious while others were slightly deformed. Although most of

Fig. 5 a Changes in micropolarity of lactoferrin-loaded liposomes formed by different chain lengths of phospholipids before and after in vitro simulated gastric fluid (SGF) and simulated intestinal fluid (SIF) digestion; **b** mechanism of micropolarity changes of liposomal membrane using pyrene as an indicator
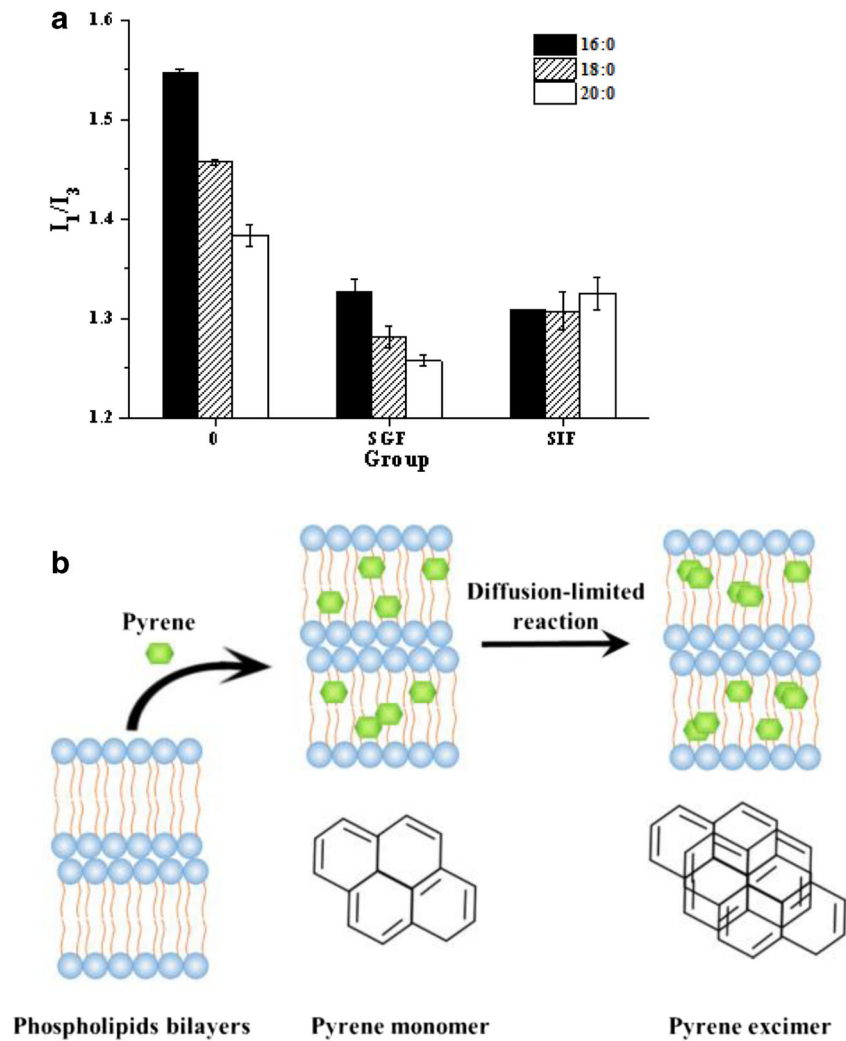


the liposomes exhibited surface deformation, they could maintain intact structure (see the arrows). However, it can be seen obviously that liposomes digested in SIF appeared irregular conformation of membranes without spherical shapes, and most of the bilayer membrane was hydrolyzed and integrated liposome structure could no longer be found. Liposomes obtained from different chain length didn't show too much difference after SIF digestion.

The acidic conditions could cause an alteration in shape of liposomes, a large proportion of the bilayer membrane could still maintain its structural integrity in SGF, indicating that the effect of low pH and pepsin on liposomes had slight effect on the membrane structure of liposomes. Besides, as shown in Fig. 2a, liposomes made from $C_{20:0}$ had larger value in z-axis, which meant the thicker membrane of this liposomes. Thus, when it shifted to the acidic environment, the deformation of $C_{20:0}$ liposomes could be more obviously. Pancreatin, contains pancreatic amylase, protease, trypsin and pancreatic lipolytic enzymes, and together with bile salts in SIF, can damage the liposomal structure through hydrolysis of the phospholipid backbone [30]. Glycerophosphoric acids and 1-acyl lysophospholipids, etc. were the products of the hydrolysis reaction during SIF digestion [45]. These by-products of lipid digestion have a further pronounced effect on destabilization of phospholipid bilayers [46]. Besides, pancreatic cholesterol esterase is known to be a bile-salt-stimulated carboxyl ester lipase that can catalyze the hydrolysis of phospholipids to release fatty acids [47]. Therefore, the products of different phospholipids digested in SIF are similar, resulting in the similar appearance of the $C_{16:0}$, $C_{18:0}$ and $C_{20:0}$ liposomes. The effect of enzymes on liposomal behavior showed much more significant than the phospholipid structure changes.

## Hydrolysis of Lactoferrin

SDS-PAGE patterns of LF-loaded liposomes with different chain lengths of phospholipids, before and after digestion in SGF and in SIF for 120 min, were presented in Fig. 7. Compared to the original samples, intact LF was found in SGF, while the LF was totally hydrolyzed after digestion in
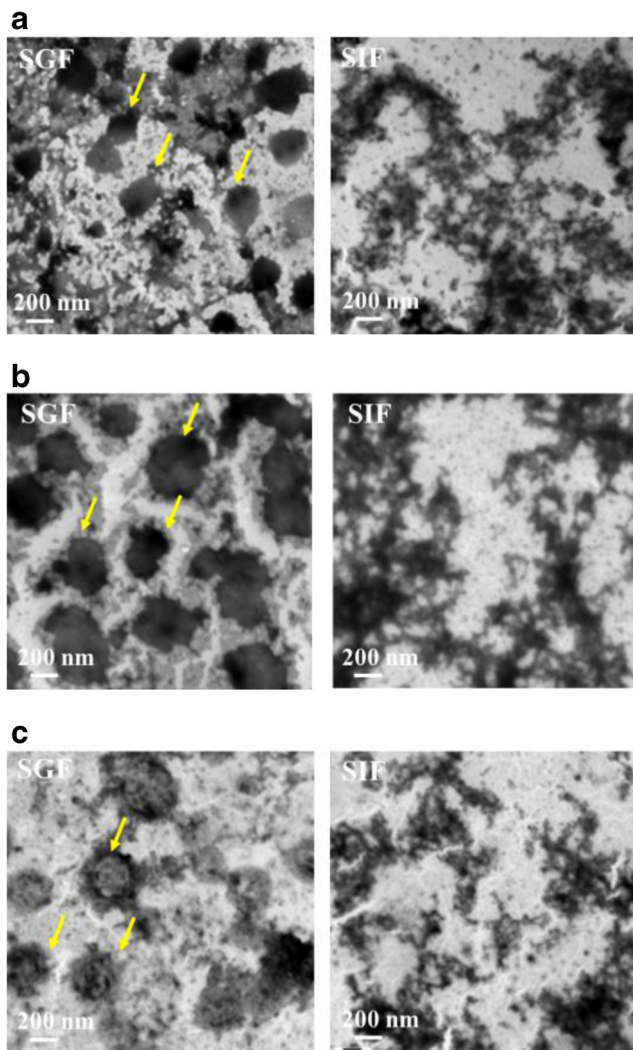
Fig. 6 Transmission electron microscopy (TEM) images of lactoferrin-loaded liposomes formed by different chain length of phospholipids after in vitro digestion in simulated gastric fluid (SGF) and simulated intestinal fluid (SIF). **a** 16:0; **b** 18:0; **c** 20:0. Arrows in the images represented the intact liposomes
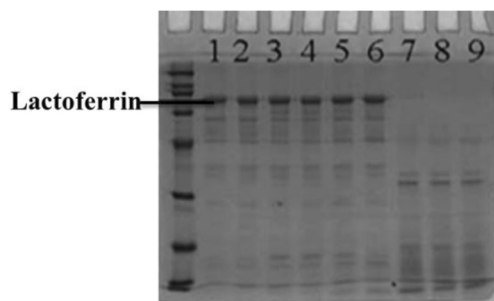


Fig. 7 Lactoferrin hydrolysis of liposomes formed by different chain lengths of phospholipids before (lane 1: $C_{16:0}$ liposome; lane 2: $C_{18:0}$ liposome; lane 3: $C_{20:0}$ liposome) and after digestion in simulated gastric fluid (SGF) (lane 4: $C_{16:0}$ liposome; lane 5: $C_{18:0}$ liposome; lane 6: $C_{20:0}$ liposome) and in simulated intestinal fluid (SIF) (lane 7: $C_{16:0}$ liposome; lane 8: $C_{18:0}$ liposome; lane 9: $C_{20:0}$ liposome) for 120 min

SIF for 120 min. The liposomes formed by $C_{16:0}$, $C_{18:0}$ and $C_{20:0}$ had the similar behavior during digestion. It seemed that the bilayer structure of the liposomes was not damaged by the low pH conditions (~3.0) and the pepsin enzyme, that the well-organized phospholipid membrane prevented pepsin from permeating into the core of liposome to hydrolyze the entrapped LF. Similar results have been reported by Bardonnet et al. [48], who found that liposomes were stable under simulated gastric conditions, and the phospholipid structure could maintain integrated. Smith et al. [49] also reported that the membrane can prevent pepsin from digestion and 80% of the original encapsulated alkaline phosphatase could maintain stable. These results were corresponding to our previous study [50], and also was in accord with the observation obtained by TEM. It indicated that different structure of phospholipids had slightly influence on digestion behavior of liposomes, which are negligible compared to the effects of enzymes on liposomes. The LF almost hydrolyzed after digesting in SIF, which means that liposomal structure decomposes under the hydrolysis of pancreatic lipase, phospholipase $A_2$ [45] and the co-effective damage function of bile salts [47] on the structure of liposomes, releasing LF from liposomal membrane and hydrolyzing by trypsin in pancreatin [51].

## Conclusions

This study has systematically demonstrated the physicchemical stability of liposomes formed by different type of phospholipids before and after in vitro digestion. The main finding in current study are as follows. (i) The micropolarity of liposomes increased (from $1.4 \pm 0.1$ to $1.6 \pm 0.1$) with the decrease of chain lengths of phospholipids ($C_{20:0}$, $C_{18:0}$, $C_{16:0}$), and micropolarity tend to decrease (from $1.5 \pm 0.1$ to $1.2 \pm 0.1$) with the increasing of liposomal unsaturation degree ($C_{18:0}$, $C_{18:1}$, $C_{18:2}$, $C_{18:3}$). (ii) The average particle diameter, surface charge, morphology, structure integrity and the release of lactoferrin of all liposomes were slight influenced in SGF, however, their structure were all altered as a function of pancreatin and bile salts after in SIF digestion. (iii) The different phospholipids structure may cause some differences in liposomal digestion behavior (rough surface and micropolarity), but it was negligible compared to the effect of enzymes and bile salts. Besides, this study also provided insight into the morphology and membrane integrity of liposomes during digestion, which may give assistance in the development of stable liposomes in vivo based on food-grade materials.

# References

1. S. Deshpande, C. Dekker, Nat. Protoc. **13**(5), 856–874 (2018)
2. A. Laouini, C. Jaafar-Maalej, I. Limayem-Blouza, S. Sfar, C. Charcosset and H. Fessi, J. Colloid. Sci. Biotechnol. **1**(2), 147–168 (2012)
3. C. Sebaaly, A. Jraij, H. Fessi, C. Charcosset, H. Greige-Gerges, Food Chem. **178**, 52–62 (2015)
4. X. Chen, D.J. Mcclements, J. Wang, et al., J. Agric. Food Chem. **66**(14), 3691–3699 (2018)
5. J. Liu, W. Liu, L.J. Salt, M.J. Ridout, Y. Ding and P.J. Wilde, J. Agric. Food Chem. **67**(1), 452–462 (2018)
6. D.J. McClements, J. Food Sci. **80**(7), N1602–N1611 (2015)
7. F.C. Lam, S.W. Morton, J. Wyckoff, T.L. Vu Han, M.K. Hwang, A. Maffa, E. Balkanska-Sinclair, M.B. Yaffe, S.R. Floyd, P.T. Hammond, Nat. Commun. **9**(1), 1991 (2018)
8. D. Choi, S.G. Min, Y.J. Jo, J. Food Biochem. **42**(1), e12464 (2018)
9. M. Huang, E. Su, F. Zheng, C. Tan, Food Funct. **8**(9), 3198–3208 (2017)
10. L. Ramezanzade, S.F. Hosseini, M. Nikkhah, Food Chem. **234**, 220–229 (2017)
11. S. Peng, L. Zou, W. Liu, Z. Li, W. Liu, X. Hu, X. Chen, C. Liu, Carbohydr. Polym. **156**, 322–332 (2017)
12. W. Liu, M. Tian, Y. Kong, J. Lu, N. Li, J. Han, LWT Food Sci. Technol. **75**, 608–615 (2017)
13. M. Marsanasco, A.L. Márquez, J.R. Wagner, S.d.V. Alonso, N.S. Chiaramoni, Food Res. Int. **44**(9), 3039–3046 (2011)
14. W. Liu, W. Liu, A. Ye, S. Peng, F. Wei, C. Liu, J. Han, Food Chem. **196**, 396–404 (2016)
15. K. Abe, K. Higashi, K. Watabe, A. Kobayashi, W. Limwikrant, K. Yamamoto, K. Moribe, Colloids Surf. A Physicochem. Eng. Asp. **474**, 63–70 (2015)
16. M. Frenzel, A. Steffen-Heins, Food Chem. **173**, 1090–1099 (2015)
17. R. Phillips, T. Ursell, P. Wiggins, P. Sens, Nature **459**(7245), 379–385 (2009)
18. M.J. Tapia, M. Monteserin, H.D. Burrows, J.S. Seixas de Melo, J. Estelrich, Photochem. Photobiol. **89**(6), 1471–1478 (2013)
19. L. Zhao, F. Temelli, J.M. Curtis, L. Chen, Food Res. Int. **77**, 63–72 (2015)
20. W. Liu, Y. Kong, P. Tu, J. Lu, C. Liu, W. Liu, J. Han, J. Liu, Food Funct. **8**(4), 1688–1697 (2017)
21. L. Zou, S. Peng, W. Liu, X. Chen, C. Liu, Food Res. Int. **69**, 114–120 (2015)
22. W. Liu, A. Ye, F. Han, J. Han, Adv. Colloid Interf. Sci. **263**, 52–67 (2019)
23. W. Liu, A. Ye, C. Liu, W. Liu, H. Singh, Food Res. Int. **48**(2), 499–506 (2012)
24. W. Liu, A. Ye, W. Liu, C. Liu, H. Singh, J. Dairy Sci. **96**(4), 2061–2070 (2013)
25. W. Liu, F. Wei, A. Ye, M. Tian, J. Han, Food Chem. **230**, 6–13 (2017)
26. M. Tian, J. Han, A. Ye, W. Liu, X. Xu, Y. Yao, K. Li, Y. Kong, F. Wei, W. Zhou, J. Sci. Food Agric. **99**(6), 2677–2684 (2019)
27. B. Maherani, E. Arab-Tehrany, A. Kheirolomoom, D. Geny, M. Linder, Biochimie **95**(11), 2018–2033 (2013)
28. L.G. Hermida, M. Sabés-Xamaní and R. Barnadas-Rodríguez, J. Liposome Res. **19**(3), 207–219 (2009)
29. W.A. Birru, D.B. Warren, A. Ibrahim, H.D. Williams, H. Benameur, C.J.H. Porter, D.K. Chalmers, C.W. Pouton, Mol. Pharm. **11**(8), 2825–2834 (2014)
30. A. Rashidinejad, E.J. Birch, D.W. Everett, Food Funct. **7**(7), 3283–3294 (2016)
31. W. Liu, J. Liu, W. Liu, T. Li, C. Liu, J. Agric. Food Chem. **61**(17), 4133–4144 (2013)
32. P. Galletti, D. Malferrari, C. Samori, G. Sartor, E. Tagliavini, Colloids Surf., B **125**, 142–150 (2015)
33. M. Minekus, M. Alminger, P. Alvito, S. Ballance, T. Bohn, C. Bourlieu, F. Carrière, R. Boutrou, M. Corredig, D. Dupont, C. Dufour, L. Egger, M. Golding, S. Karakaya, B. Kirkhus, S. le Feunteun, U. Lesmes, A. Macierzanka, A. Mackie, S. Marze, D.J. McClements, O. Ménard, I. Recio, C.N. Santos, R.P. Singh, G.E. Vegarud, M.S.J. Wickham, W. Weitschies, A. Brodkorb, Food Funct. **5**(6), 1113–1124 (2014)
34. H.C. Chang, D.R. Flanagan, J. Pharm. Sci. **84**(9), 1078–1082 (1995)
35. L.H. Fasolin, R.C. Santana, R.L. Cunha, Colloids Surf. A Physicochem. Eng. Asp. **459**(459), 290–297 (2014)
36. R. Gharib, L. Auezova, C. Charcosset, H. Greige-Gerges, Food Chem. **218**, 365–371 (2017)
37. R. Lipowsky, Nature **349**(6309), 475–481 (1991)
38. K. Makino, T. Yamada, M. Kimura, T. Oka, H. Ohshima, T. Kondo, Biophys. Chem. **41**(2), 175–183 (1991)
39. A. Bootz, V. Vogel, D. Schubert, J. Kreuter, Eur. J. Pharm. Biopharm. **57**(2), 369–375 (2004)
40. U. Jakobsen, S. Vogel, Bioconjug. Chem. **24**(9), 1485–1495 (2013)
41. B.J. Berne and R. Pecora, Dynamic light scattering: with applications to chemistry, biology, and physics. Wiley, New York, pp. 206–210 (2000)
42. S. Pandey, S.N. Baker, S. Pandey, G.A. Baker, J. Fluoresc. **22**(5), 1313–1343 (2012)
43. Z.S. Haidar, R.C. Hamdy, M. Tabrizian, Biomaterials **29**(9), 1207–1215 (2008)
44. S. Nguyen, S.J. Alund, M. Hiorth, A.L. Kjøniksen, G. Smistad, Colloids Surf., B **88**(2), 664–673 (2011)
45. S. Gallier, E. Shaw, J. Cuthbert, D. Gragson, H. Singh, R. Jiménez-Flores, Food Res. Int. **54**(1), 718–725 (2013)
46. G. Peng, Y. Du, Y. Wei, J. Tang, A.Y. Peng, L. Rao, Org. Biomol. Chem. **9**(7), 2530–2534 (2011)
47. L. Yang, F. Feng, J.P. Fawcett, I.G. Tucker, J. Liposome Res. **25**(1), 58–66 (2014)
48. P.L. Bardonnet, V. Faivre, P. Boullanger, M. Ollivon, F. Falson, Biochem. Biophys. Res. Commun. **383**(1), 48–53 (2009)
49. A.M. Smith, M.R. Jaimefonseca, L.M. Grover, S. Bakalis, J. Agric. Food Chem. **58**(8), 4719–4724 (2010)
50. W. Liu, A. Ye, W. Liu, C. Liu, J. Han, H. Singh, Food Chem. **175**, 16–24 (2015)
51. R. Nilisha, N. Nitish, A. Hammad, et al., PLoS One **9**(3), e90011 (2014)